Shallow remineralization in the Sargasso Sea estimated from seasonal variations in oxygen and dissolved inorganic carbon

S. Ono[1], A. Ennyu[1], R. G. Najjar[1], N. Bates[2]

[1]*Department of Geosciences, The Pennsylvania State University, University Park, PA 16802, U.S.A.*

[2]*Bermuda Biological Station for Research, Inc. 17 Biological Lane, Ferry Reach GE 01 Bermuda*

October 16, 1998

Submitted to Deep-Sea Research

Abstract

A diagnostic model of the mean annual cycles of dissolved inorganic carbon (DIC) and oxygen below the mixed layer at the Bermuda Atlantic Time-series Study (BATS) site is presented and used to estimate organic carbon remineralization in the seasonal thermocline. The model includes lateral and vertical advection as well as vertical diffusion. Very good agreement is found for the remineralization estimates based on oxygen and DIC. Net remineralization averaged from mid-spring to early fall is found to be a maximum between 120 and 140 m. Remineralization integrated between 100 (the compensation depth) and 250 m during this period is estimated to be about 1 mol C m^{-2}. This flux is consistent with independent estimates of the loss of particulate and dissolved organic carbon.

1. Introduction

The ocean's "biological pump," characterized by net production of organic matter in surface waters and net remineralization in deeper waters, maintains vertical gradients in a myriad of chemical species in the sea. Much attention has been paid to the production side of the pump but relatively little is known about remineralization, particularly at shallow depths, where it is suspected that most of the remineralization occurs. Large mesoscale

variability and problems with sediment traps have made the task of estimating shallow remineralization a frustrating one.

Here we exploit the measured seasonal variations in oxygen and dissolved inorganic carbon (DIC) at the Bermuda Atlantic Time-series Study (BATS site: Figure 1) in order to estimate shallow remineralization. To our knowledge, only one study has used seasonal variations in oxygen for this purpose (JENKINS and GOLDMAN, 1985) and none have used seasonal variations in DIC. To avoid the difficulties of estimating the impact of mixed layer entrainment on these seasonal variations, we focus our attention on the period from May through October, when the mixed layer is shoaling or only slightly deepening. We do consider, however, vertical mixing in the seasonal thermocline, as well as vertical and lateral advection. The basic approach is to estimate lateral advection from climatological estimates of the geostrophic flow, vertical advection from the Ekman balance, and then to tune the vertical diffusivity to best match the temperature distribution. Remineralization is then determined diagnostically from the oxygen and DIC budgets.

The main data sets we draw on in this study are the temperature, DIC and oxygen measurements made at the BATS site, in addition to measurements of these variables (and salinity) from "validation cruises" (Figure 1). The latter, together with climatological estimates of temperature and salinity, are used to estimate lateral advection of heat, DIC and oxygen.

2. Mean annual cycles of oxygen and DIC

BATS core data from 1989 to 1996 were used to construct mean annual cycles of temperature (T), salinity (S), oxygen, and DIC. In order to obtain smooth annual cycles for the time rate of change, the annual cycles of each property at depths of 2.5, 10, 20, 40, 60, 80, 100, 140, 160, 200 and 250 m were constructed by using a weighted moving average. The discrete data were averaged using a weighting factor with a normal distribution:

$$\gamma_n(t) = \frac{1}{2\sqrt{\pi}} \exp\left[-\left(\frac{t_n - t}{2\sigma}\right)^2\right], \qquad (1)$$

where t is time, n is the index of the discrete data point and σ is a time scale for averaging. We chose σ to be 25 days at 2.5 m, increasing gradually to 40 days at 250 m. The averaging window is half of a year.

The time averaged data of T, S and DIC were fit vertically by using the sigmoid function of GOYET and DAVIS (1997) in order to obtain smooth depth derivatives. The sigmoid function we used has the form:

$$C(z) = a_1 + b_1 z + \frac{c_1}{\left[1 + \exp(-d_1(x - e_1))\right]^{f_1}}, \qquad (2)$$

where a_1, b_1, c_1, d_1, e_1 and f_1 are parameters obtained by least squares fit. Since the oxygen depth profile exhibits a subsurface oxygen maximum from summer to fall, it was fit by least squares using:

$$O_2(z) = a_2 + b_2 z + c_2 \exp(-d_2 z) + \exp(-e_2 (z - f_2)^2), \qquad (3)$$

where a_2, b_2, c_2, d_2, e_2 and f_2 are fitting parameters.

Figure 2 shows the computed time rate of change of dissolved oxygen and DIC. The dashed lines indicate the depth at which the temperature differs by 2 °C and 1.5 °C from the surface temperature. We will focus on the water column below this layer and above 250 m, considering it to be the stratified seasonal thermocline, in which wind-driven

mixing is not the dominant process driving vertical transport. This layer is deeper than that of the conventionally defined mixed layer depth (e.g. GRUBER *et al.*, 1998).

In surface waters (0-30 m), oxygen and DIC are in phase. Both oxygen and DIC increase during fall and winter, and decrease during spring and summer (Figure 2). DIC is largely affected by vertical exchange and biological processes, whereas oxygen is affected mainly by air-sea gas transfer.

In deeper water (~150 m), DIC and oxygen are out of phase. Since shallow water is high in oxygen and low in DIC compared to deep water, oxygen increases and DIC decreases in deeper water in winter when the mixed layer deepens. The rates of change of DIC and oxygen during this period are similar, with a maximum rate of 0.08 mmol m^{-3} day^{-1}. Following stratification in spring, biological remineralization of organic matter increases DIC and decreases oxygen. Again, the time rate of change of oxygen and DIC are similar, with a maximum rate of ~0.04 mmol m^{-3} day^{-1} at ~150 m depth during summer.

3. Model formulation

The general form of tracer conservation used here is

$$\frac{\partial C}{\partial t} = -u\frac{\partial C}{\partial x} - v\frac{\partial C}{\partial y} - w\frac{\partial C}{\partial z} - \frac{\partial}{\partial z}\left(K\frac{\partial C}{\partial z}\right) + J_C \quad , \qquad (4)$$

where C represents temperature, DIC concentration or oxygen concentration; u, v and w are the velocity components; K is the vertical diffusivity and J_C is an internal source term. For temperature, J_C represents the effect of solar radiation that penetrates below the mixed layer. For oxygen and DIC, J_C represents the net effects of photosynthesis and respiration.

The surface solar radiation is specified as a simple sinusoidal function fit from data of MUSGRAVE *et al.* (1988). The mean and amplitude are set to be 180 and 80 W m^{-2},

respectively, and the maximum occurs on July 13th. Following PAULSON and SIMPSON (1977), solar radiation as function of depth is parameterized as a double exponential with coefficients for Jerlov water type *I*.

Geostrophic velocities, u and v, were computed from climatological temperature and salinity data of LEVITUS AND BOYER (1994) and LEVITUS *et al.* (1994), and the thermal wind equations. The approach is similar to that of SIEGEL AND DEUSER (1997). To obtain the seasonality of lateral advection, we used the "seasonal" (three-month averaged) data. The four grid points surrounding the BATS site were selected (Figure 1). The density of water was calculated using the formulation of MILLERO AND POISSON (1981), and longitudinal and latitudinal density gradients were computed using averaged density for each x and y component. Velocities were computed for the upper 250 m assuming a level of no motion at 3000 m. The four seasonal values of velocities and T and S gradients were fit with a single harmonic to obtain values every 5 days. The calculated geostrophic flow is from northeast to southwest at the rate of 0.02 to 0.03 m s^{-1}, consistent with the calculation of SIEGEL AND DEUSER (1997).

The horizontal gradients of oxygen and DIC were estimated from BATS validation cruise data. We assumed a simple linear relationship between the horizontal gradient of oxygen (and DIC) and temperature and salinity. That is,

$$\Delta O_2 \text{ (or } \Delta DIC) = \alpha\, \Delta T + \beta\, \Delta S \ , \qquad (5)$$

where ΔO_2, ΔDIC, ΔT, and ΔS represent the difference between each cast data and the cast closest to the BATS site. α and β are the coefficients which are determined by least squares fit as a function of depth but independent of time. Both ΔO_2 and ΔDIC correlate well with ΔS and ΔT in surface waters (0 to 100 m, r = 0.9 to 0.5, N $\approx$ 30), indicating air-sea gas

exchange and evaporation/precipitation processes dominate oxygen and DIC variations. However, the goodness of fit decreases with increasing depth (for 100 to 250 m, $r \approx 0.3$, $N \approx 30$), indicating that mesoscale eddy or biological processes predominate. The uncertainty in the advection of oxygen and DIC may be large.

Ekman downwelling is an important mechanism for vertical transport in the Sargasso Sea (MUSGRAVE *et al.*, 1988). We used the simple harmonic function of DONEY *et al.* (1996) to compute the Ekman downwelling velocity: the amplitude and the annual mean are 34.6 m $year^{-1}$ and 60 m $year^{-1}$, respectively, and the maximum value is on January 1st. The Ekman downwelling velocity is set to be zero at the surface and increases linearly to the Ekman depth, which is taken to be 30 m (PRICE *et al.*, 1987), and decreases linearly to zero at 250 m.

The time rate change of temperature was prognostically modeled using Equation (4) in order to estimate an appropriate diffusivity. In the stably stratified thermocline, GASPER *et al.* (1990) and GARGETT and HOLLOWAY (1984) suggest that $K = AN^{-1}$, where N is the Brunt-Väisälä frequency. Since salinity variations are small, we computed N as a function of T only, using a constant expansion coefficient of -0.15 kg m^{-3} $°C^{-1}$. We chose $A = 4.2 \times 10^{-7}$ s m^{-1}, which is larger than that of GASPER *et al.* (1990) by a factor of three, for the best fit to the temperature distribution. The corresponding diffusivity is calculated to be from 1.5×10^{-5} to 6×10^{-5} m^2 s^{-1}, decreasing towards the surface.

The model simulates the time rate of change of temperature well in the thermocline during spring and summer (Figure 3). Since the estimated diffusivity only applies to the seasonal thermocline, the model does not produce the observed time rate of change of temperature during winter, when wind driven mixing is predominant.

4. Remineralization rate in thermocline

The biological flux terms for oxygen (J_{O2}) and DIC (J_{DIC}) determined diagnostically from Equation (4) are shown in Figure 4. J_{O2} was converted to carbon units using an O_2:C Redfield ratio of -138:103. In the seasonal thermocline, J_{O2} and J_{DIC} are generally consistent. J_{O2} shows a maximum respiration at 120 m in spring to fall of 0.08 mmol C m^{-3} day^{-1}. J_{DIC} also shows a respiration maximum of 0.08 mmol C m^{-3} day^{-1} but slightly deeper (150 m). The compensation depth, at which photosynthesis is equal to respiration, is between 90 and 100 m from spring to fall. The time averaged J_{O2} and J_{DIC} for the same period are remarkably similar between 70 and 250 m (Figure 5).

The modeled oxygen and DIC budget averaged Julian day from 129 to 289 (May 9th to October 16th) shows that the vertical diffusion rate is estimated to be as large as the time rate of change of oxygen and DIC between 100 and 250 m depth (Figure 6). The Ekman transport term becomes important above 150 m depth. The horizontal advection term, although somewhat uncertain, is estimated to be small compared to the other terms. However, the advective term becomes important at ~200 m because the other terms become relatively small.

Figure 7 summarizes the integrated oxygen and DIC budget between 100 and 250 m depth obtained in this study for the period between May 9th and October 16th. The consumption of oxygen by remineralization is twice as large as the net oxygen loss for this water column. Vertical transport, both by Ekman downwelling and eddy diffusion, is a source of oxygen. The DIC budget shows a DIC gain by remineralization (0.94 mol C m^{-2}) that is twice as large as the DIC change. Vertical diffusion and Ekman transport are sinks of DIC. Given the O_2:C stoichiometry assumed here, the simulated oxygen sink by remineralization (-1.21 mol O_2 m^{-2}) is essentially equivalent to the integrated remineralization rate estimated by DIC budget (+0.94 mol C m^{-2}).

5. Discussion

Remineralization rates in the Sargasso Sea from a variety of tracer-based techniques were summarized by SARMIENTO *et al.* (1990). Between 100 and 250 m, these rates vary from about 0.6 to 3.3 mol O_2 m^{-2} yr^{-1}. Assuming, crudely, that half of the annual respiration occurs in the 160 day period considered here, our estimate of 1.2 mol O_2 m^{-2} for this time period is bracketed by this range (0.3 to 1.7 mol O_2 m^{-2}). JENKINS and GOLDMAN (1985) estimated remineralization in the Sargasso Sea for roughly the same time period based on seasonal variations in the oxygen anomaly (the departure from saturation). The integrated remineralization from 100 to 250 m based on their analysis is 1.7 mol O_2 m^{-2}, somewhat larger than our estimate. Our results also differ from JENKINS and GOLDMAN (1985) in terms of the remineralization length scale. A least squares exponential fit to the remineralization rates in Figure 5 from the depth of the maximum to 250 m yields *e*-folding length scales of 44 and 60 m for J_{DIC} and J_{O2}, respectively. This is much shorter than the 260 m length scale inferred by JENKINS and GOLDMAN (1985). JENKINS and GOLDMAN (1985) did not consider seasonal variations in the oxygen anomaly due to advection and diffusion, and this may account for the difference with our estimate.

The remineralization rate estimated here can also be compared to new production estimates. A compilation by GRUBER *et al.* (1998) gave a range of 2 to 4 mol C m^{-2} yr^{-1}. Thus, 25 to 50% of the annual new production is remineralized between 100 and 250 m from late spring to early fall.

Because dissolved and particulate organic carbon (DOC and POC, respectively) are lost from surface waters in very different ways, it is of interest to determine their relative importance in export and remineralization. CARLSON *et al.* (1994) found that DOC integrated between 100 and 250 m at the BATS site decreased by about 1 mol C m^{-2} from late spring to early fall. However, more than half of the DOC was consumed by the end of April. Thus, from May to October, DOC would account for about half of the remineralization estimated in this study.

Particulate organic carbon fluxes have been measured in sediment traps at the BATS site at the depths of 150, 200 and 300 m. We integrated POC data (from 1989 to 1996) for the 160 day period of interest at these three depths. Estimates at 250 m were made by linear interpolation and at 100 m by multiplying the flux at 150 m by 1.5, following the MARTIN *et al.* (1987) flux scaling. The decrease in the flux from 100 to 250 m is obtained to be 0.26 mol C m^{-2} for the period of interest, about ~28% of the net remineralization estimated here. However, MICHAELS *et al.* (1994) suggest that the sediment traps at the BATS site may underestimate the POC flux by about a factor of two. The contribution of POC to the net remineralization may, therefore, be as large as ~56%. Therefore, the ratio of DOC to POC remineralized between 100 and 250 m during the period of interest is estimated to be roughly to 1:1 to 2:1.

Even though more improvement is needed in quantifying transport processes, this study suggests that such processes are important for characterizing temporal variations of oxygen and DIC in the seasonal thermocline. It is likely that other biologically important variables, such as nutrients, POC and DOC are similarly affected. The approach taken here could be extended to these variables to improve our understanding of the biogeochemistry of the shallow aphotic zone.

Acknowledgments -- We wish to thank all the researchers at BBSR who made this study possible by creating a high quality data set and making it readily accessible. We wish to thank Dr. H. Ohmoto and Dr. M. A. Arthur for their encouragement and support for this study. This research is supported by NASA Grant #NAD5-6451 to R. G. Najjar. A. Ennyu is supported by a graduate fellowship program of Yoshida Scholarship Foundation, YKK Corporation.

REFERENCES

CARLSON, C. A., H. W. DUCKLOW, and A. F. MICHAELS (1994) Annual flux of dissolved organic carbon from the euphotic zone in the northwestern Sargasso Sea. *Nature*, **371**, 405-408.

DONEY, S. C., D. M. GLOVER, and R. G. NAJJAR (1996) A new coupled, one-dimensional biological-physical model for the upper ocean: Applications to the JGOFS Bermuda Atlantic Time-series Study (BATS) site. *Deep Sea Research II*, **43**, 591-621.

GARGETT, A. E. and G. HOLLOWAY (1984) Dissipation and diffusion by internal wave breaking. *Journal of Marine Research*, **42**, 15-27.

GASPER, P., Y. GRÉGORIS, and J.-M. LEFEVRE (1990) A simple Eddy kinetic energy model for simulations of the ocean vertical mixing: Tests at Station Papa and long-term upper ocean study site. *Journal of Geophysical Research*, **95**, 16179-16193.

GOYET, C. and D. DAVIS (1997) Estimation of total CO_2 concentration throughout the water column. *Deep-Sea Research*, **44**, 859-877.

GRUBER, N., C. D. KEELING, and T. F. STOCKER (1998) Carbon-13 constraints on the seasonal inorganic carbon budget at the BATS site in the northwestern Sargasso Sea. *Deep-Sea Research I*, **45**, 673-717.

JENKINS, W. J. and J. C. GOLDMAN (1985) Seasonal oxygen cycling and primary production in the Sargasso Sea. *Journal of Marine Research*, **43**, 465-491.

LEVITUS, S. and T. BOYER (1994) *World Ocean Atlas 1994 Volume 4: Temperature.* NOAA Atlas NESDIS 4, U.S. Department of Commerce, Washington, D.C., pp. 117.

LEVITUS, S., R. BURGETT, and T. BOYER (1994) *World Ocean Atlas 1994 Volume 3: Salinity.* NOAA Atlas NESDIS 3, U.S. Department of Commerce, Washington, D.C., pp. 99.

MARTIN, J. H., G. A. KNAUER, D. M. KARL, and W. W. BROENKOW (1987) VERTEX: carbon cycling in the northeast Pacific. *Deep-Sea Research*, **34**, 267-285.

MICHAELS, A. F., N. R. BATES, K. O. BUESSELER, C. A. CARLSON, and A. H. KNAP (1994) Carbon-cycle imbalances in the Sargasso Sea. *Nature*, **372**, 537-540.

MILLERO, F. J. and A. POISSON (1981) International one-atmosphere equation of state of seawater. *Deep-Sea Research*, **28A**, 625-629.

MUSGRAVE, D. L., J. CHOW, and W. J. JENKINS (1988) Application of a model of upper-ocean physics for studying seasonal cycles of oxygen. *Journal of Geophysical Research*, **93**, 15679-15700.

PAULSON, C. A. and J. J. SIMPSON (1977) Irradiance measurements in the upper ocean. *Journal of Physical Oceanography*, **7**, 952-956.

PRICE, J. F., R. A. WELLER, and R. R. SCHUDLICH (1987) Wind-driven ocean currens and Ekman transport. *Science*, **238**, 1534-1538.

SARMIENTO, J. L., G. THEILE, R. M. KEY, and W. S. MOORE (1990) Oxygen and nitrate new production and remineralization in the North Atlantic subtropical gyre. *Journal of Geophysical Research*, **95**, 18303-18315.

SIEGEL, D. A. and W. G. DEUSER (1997) Trajectories of sinking particles in the Sargasso Sea: modeling of statistical funnels above deep-ocean sediment traps. *Deep-Sea Research I*, **44**, 1519-1541.

Figure Captions

Figure 1. Map showing location of BATS validation cruises between January 93 and October 95 and the grid points of the climatological temperature and salinity data used in this study.

Figure 2. Mean annual cycles of the time rates of change of oxygen (a) and DIC (b). Dashed lines indicate depth at which temperature differs by 1.5 and 2 °C from the surface.

Figure 3. Observation (a) and simulated (b) time rate of change of temperature in the seasonal thermocline.

Figure 4. The biological source minus sink term of inorganic carbon modeled from the oxygen budget (a) and DIC budget (b).

Figure 5. Modeled photosynthesis minus respiration rate as a function of depth, averaged from May 9 to October 16. Dashed line: calculated from DIC budget. Solid line: calculated from oxygen budget (multiplied by -108/138).

Figure 6. Non-biological terms in the budgets of oxygen (a) and DIC (b) averaged from May 9 to October 16. $\mathbf{J}_{adv}$: advective transport, $\mathbf{J}_{ek}$: Ekman transport, $\mathbf{J}_{diff}$: vertical diffusivity.

Figure 7. DIC (left) and oxygen (right) budgets integrated from 100 to 250 m, and from May 9 to October 16).

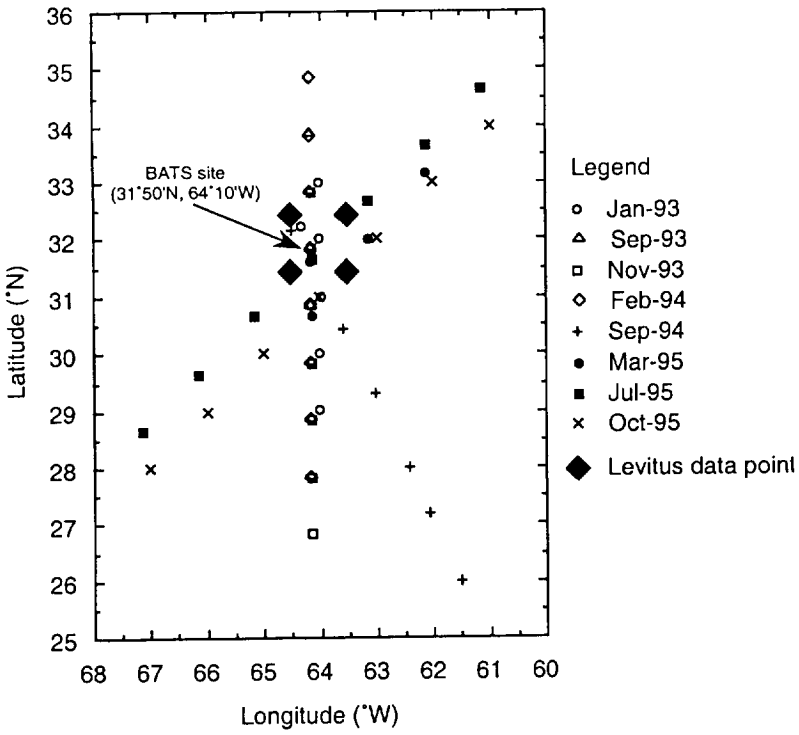
BATS site
(31°50'N, 64°10'W)
Latitude (°N)
Longitude (°W)
36
35
34
33
32
31
30
29
28
27
26
25
68
67
66
65
64
63
62
61
60
Legend
Jan-93
Sep-93
Nov-93
Feb-94
Sep-94
Mar-95
Jul-95
Oct-95
Levitus data point

Fig. 1

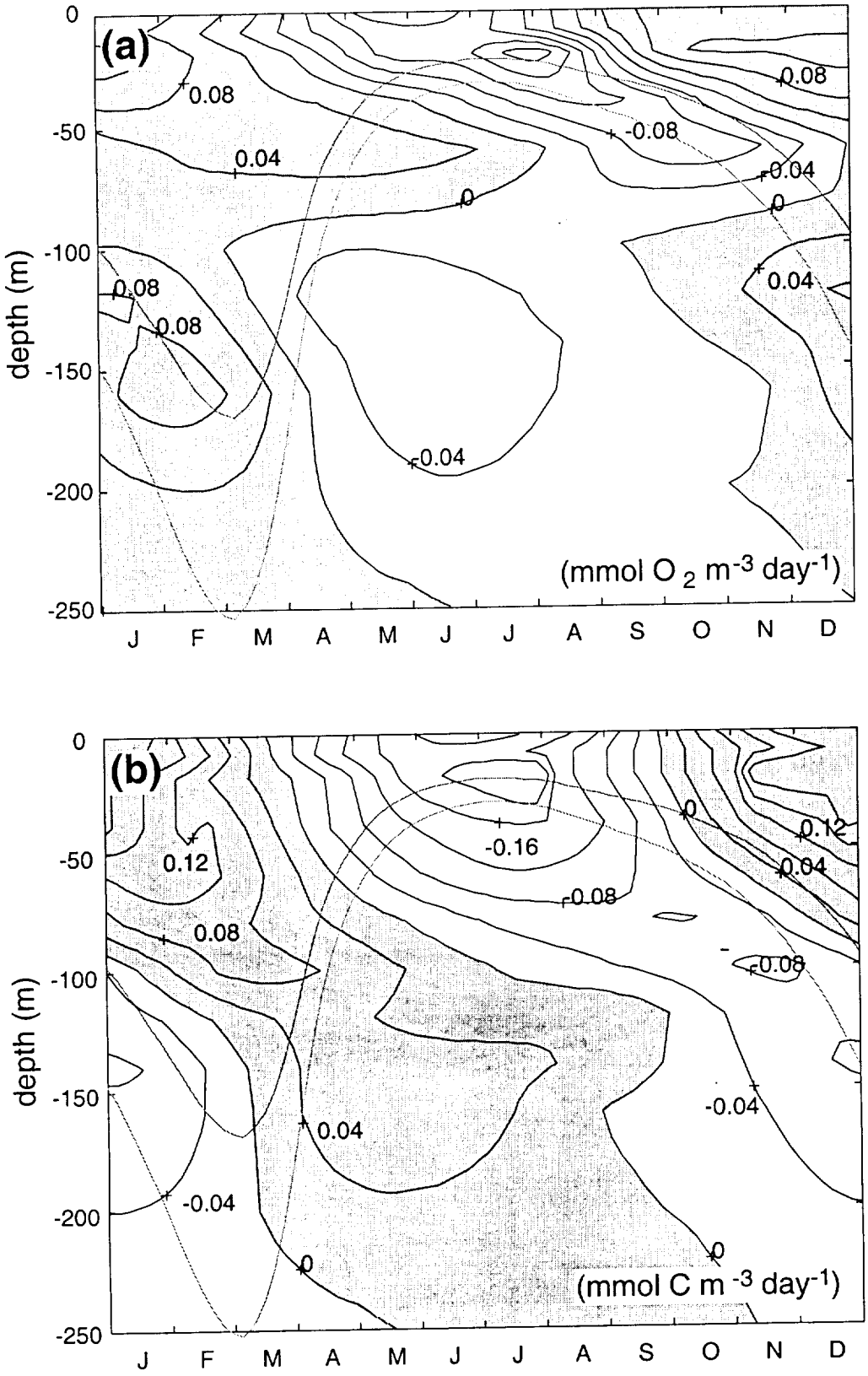
(a)
0
-50
-100
-150
-200
-250
depth (m)
0.08
0.04
0
-0.08
0.04
0
0.04
0.08
0.08
0.04
(mmol O 2 m-3 day-1)
J F M A M J J A S O N D
(b)
0
-50
-100
-150
-200
-250
depth (m)
0.12
0.08
-0.16
0
0.12
0.04
0.08
0.08
0.04
-0.04
-0.04
0
(mmol C m -3 day-1)
J F M A M J J A S O N D

Fig.2

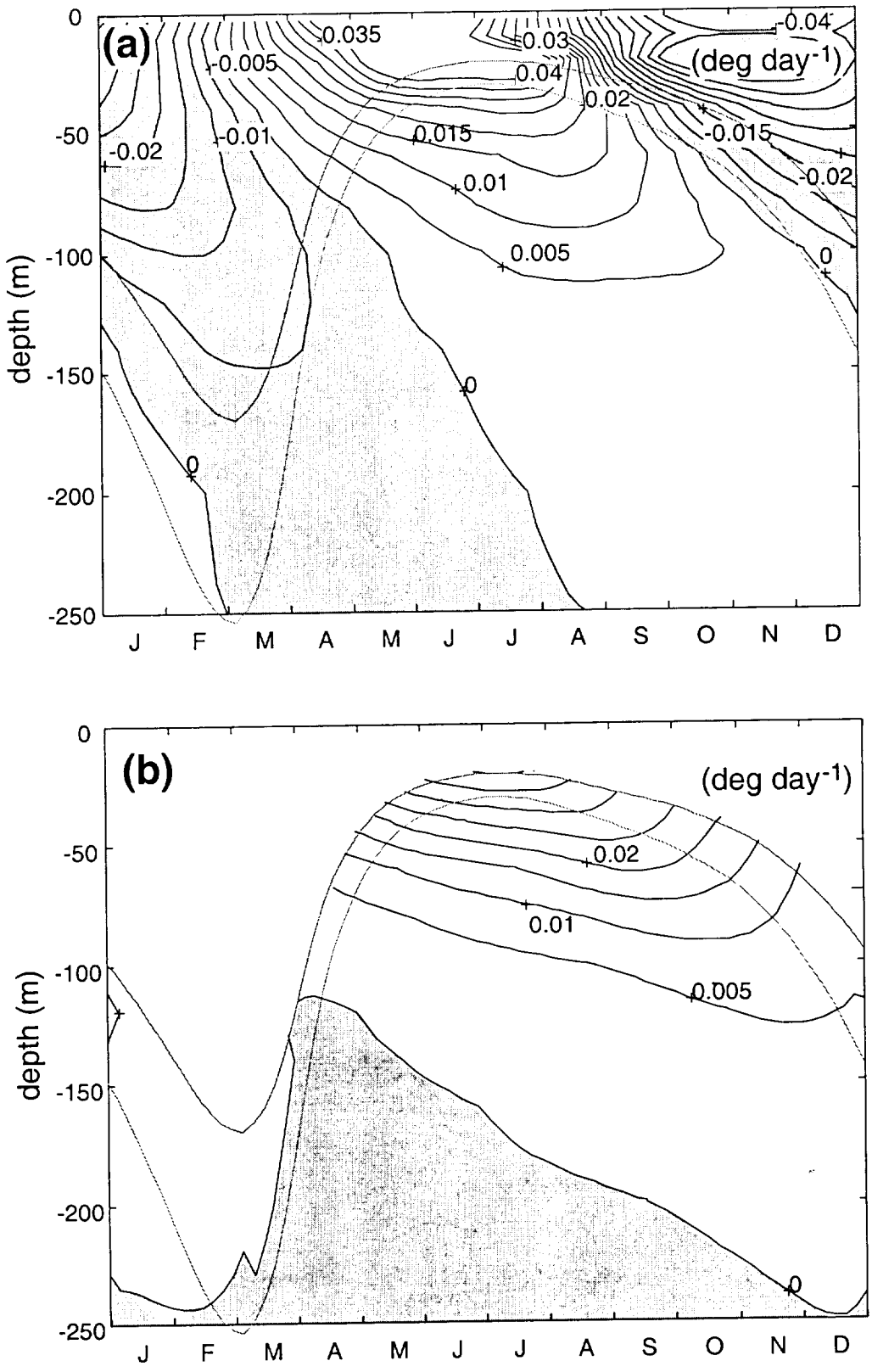
(a)
(deg day-1)
0.035
0.03
0.04
0.02
-0.04
-0.005
-0.01
0.015
-0.015
-0.02
0.01
0.005
0
depth (m)
0
-50
-100
-150
-200
-250
J F M A M J J A S O N D
(b)
(deg day-1)
0.02
0.01
0.005
0
depth (m)
0
-50
-100
-150
-200
-250
J F M A M J J A S O N D

Fig. 3

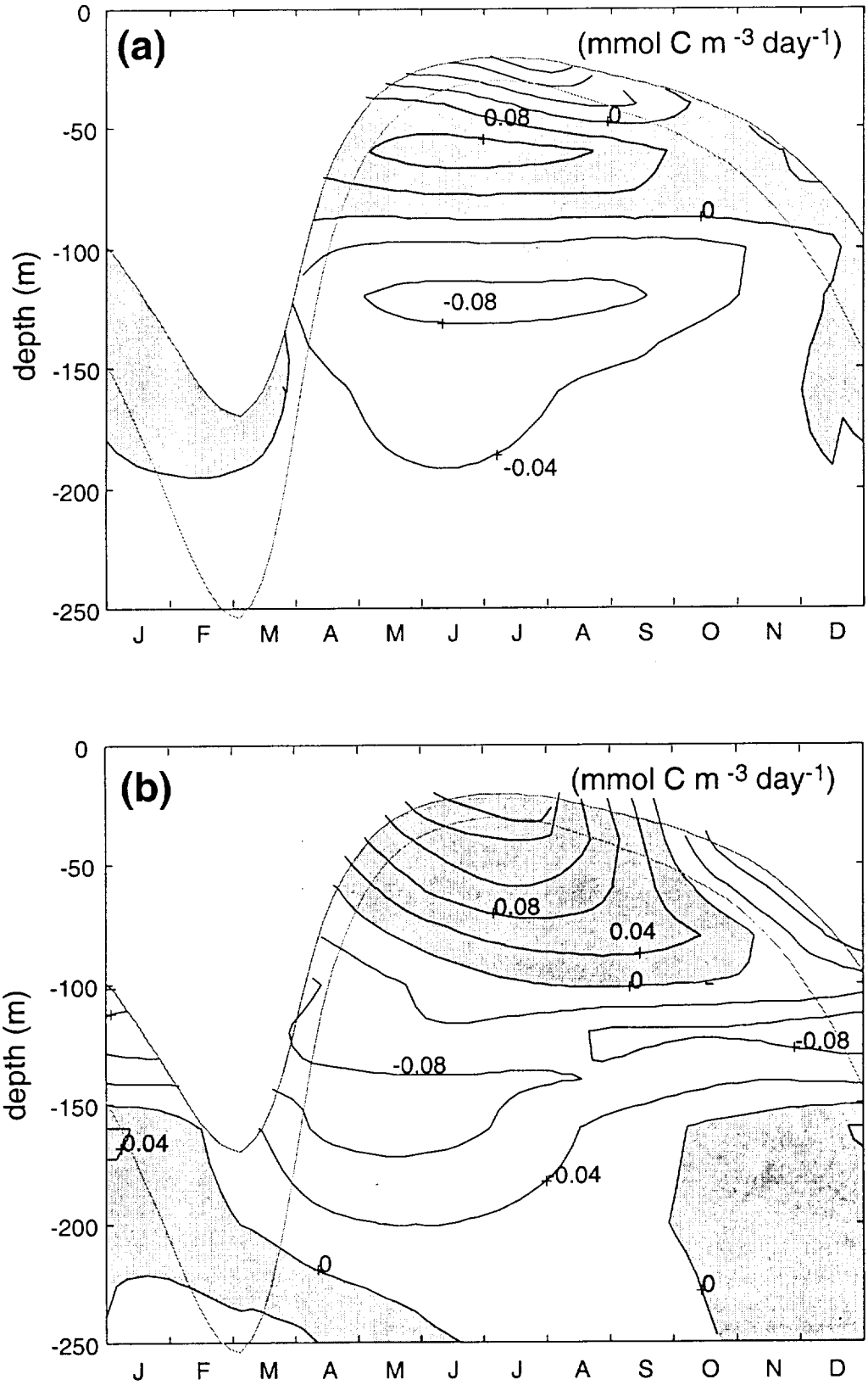
(a)
(mmol C m -3 day-1)
0.08
0
0
-0.08
-0.04
depth (m)
0
-50
-100
-150
-200
-250
J F M A M J J A S O N D
(b)
(mmol C m -3 day-1)
0.08
0.04
0
-0.08
-0.08
0.04
0.04
0
0
depth (m)
0
-50
-100
-150
-200
-250
J F M A M J J A S O N D

Fig. 4

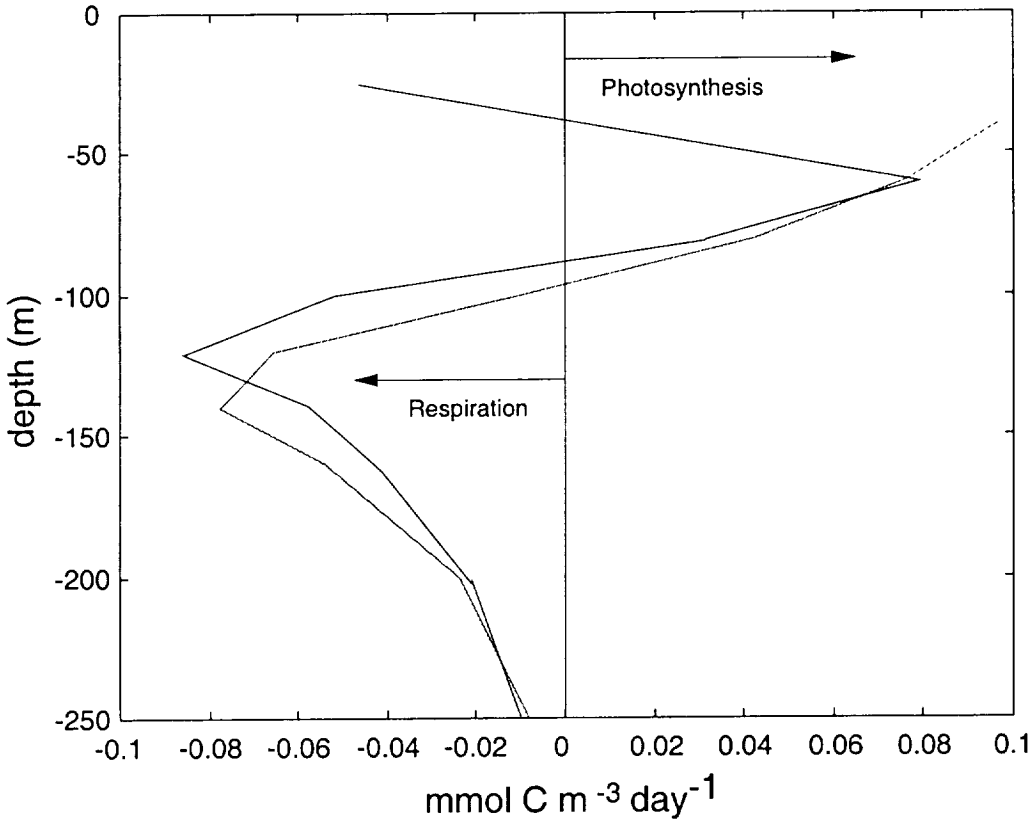
0
-50
-100
-150
-200
-250
depth (m)
Photosynthesis
Respiration
-0.1
-0.08
-0.06
-0.04
-0.02
0
0.02
0.04
0.06
0.08
0.1
mmol C m -3 day-1

Fig.5

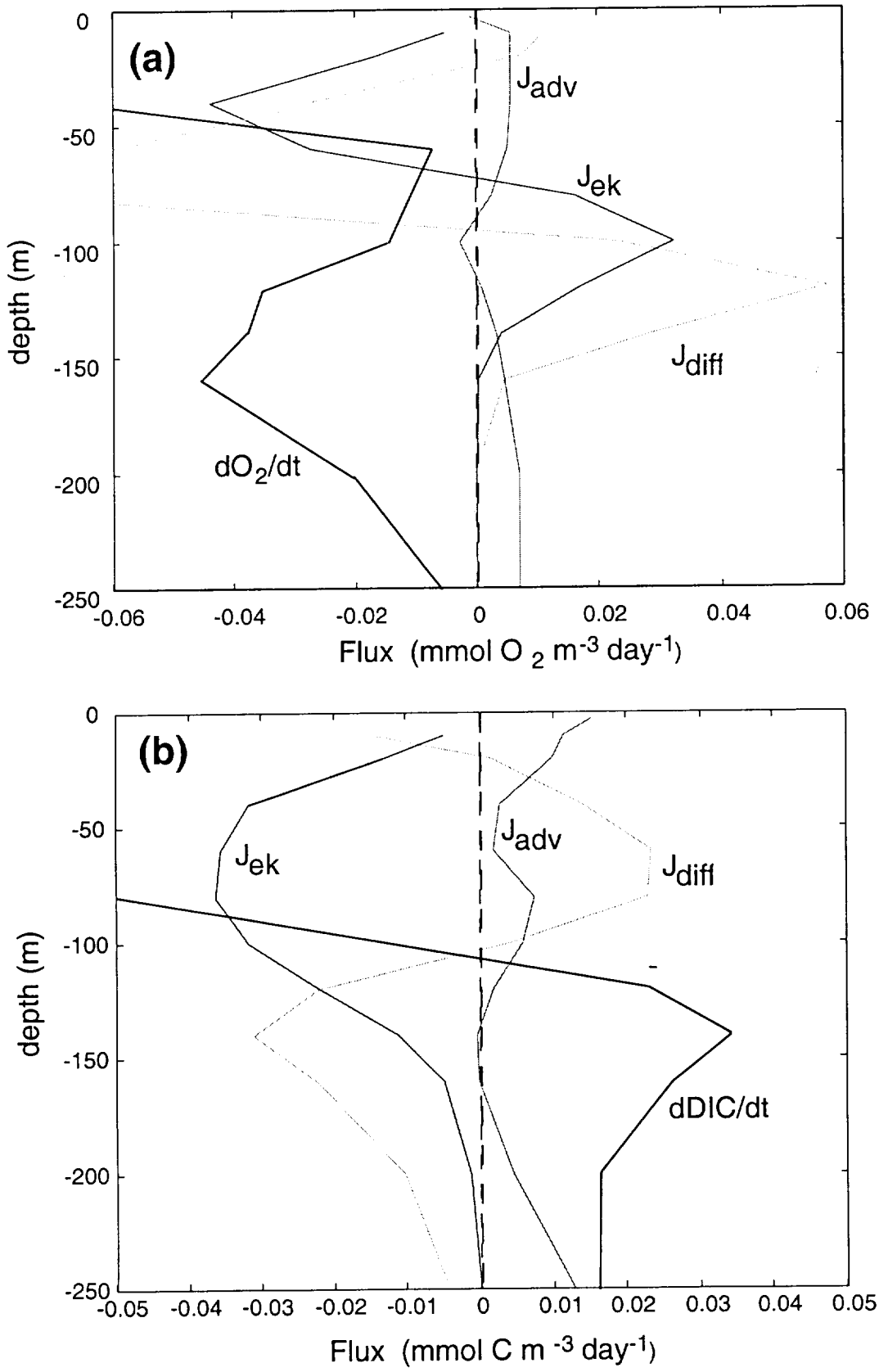
(a)
J_{adv}
J_{ek}
J_{diff}
dO_2/dt
depth (m)
0
-50
-100
-150
-200
-250
-0.06
-0.04
-0.02
0
0.02
0.04
0.06
Flux (mmol O_2 m^{-3} day^{-1})
(b)
J_{ek}
J_{adv}
J_{diff}
dDIC/dt
depth (m)
0
-50
-100
-150
-200
-250
-0.05
-0.04
-0.03
-0.02
-0.01
0
0.01
0.02
0.03
0.04
0.05
Flux (mmol C m^{-3} day^{-1})

Fig. 6

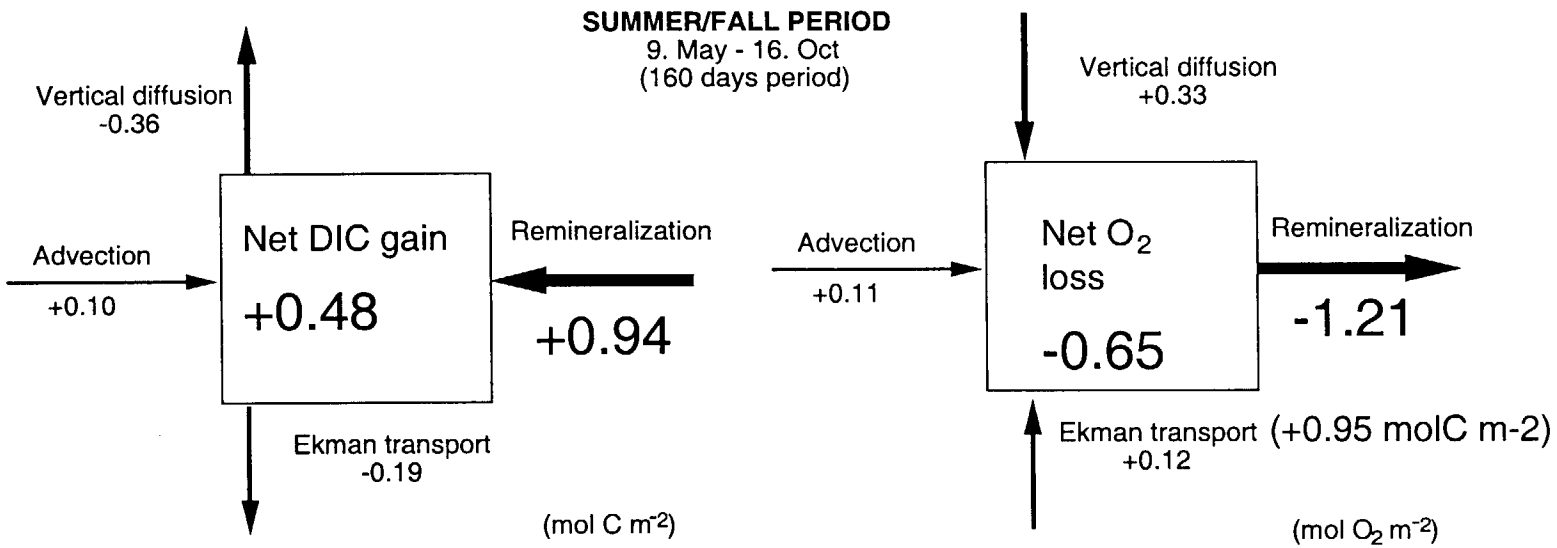
SUMMER/FALL PERIOD
9. May - 16. Oct
(160 days period)
Vertical diffusion
-0.36
Advection
+0.10
Net DIC gain
+0.48
Remineralization
+0.94
Ekman transport
-0.19
(mol C m-2)
Vertical diffusion
+0.33
Advection
+0.11
Net O2
loss
-0.65
Remineralization
-1.21
Ekman transport
+0.12
(+0.95 molC m-2)
(mol O2 m-2)

Fig.7